A Nonlinear Observer for Integration of GNSS and IMU Measurements with Gyro Bias Estimation

Håvard Fjær Grip[⋆,†], Thor I. Fossen[†], Tor A. Johansen[†], and Ali Saberi[⋆]

[⋆]School of Electrical Engineering and Computer Science, Washington State University, Pullman, WA 99164, USA
[†]Department of Engineering Cybernetics, Norwegian University of Science and Technology, 7491 Trondheim, Norway

***Abstract*— We present an observer for estimating position, velocity, attitude, and gyro bias, by using inertial measurements of accelerations and angular velocities, magnetometer measurements, and satellite-based measurements of position and (optionally) velocity. The design proceeds in two stages: in Stage I, an attitude and gyro bias estimator is designed based on an unmeasured signal. In Stage II, that design is recovered using measured signals only, by combining it with a position and velocity estimator. We prove global exponential stability of the estimation error and test the design using realistic flight simulation.**

I. Introduction

Navigation is the task of determining an object's position, velocity, or attitude by combining information from different sources. The available information varies depending on the application; however, the combination of satellite receivers, such as GPS, and inertial instruments (i.e., accelerometers and rate gyroscopes) is found in many applications, often together with additional sensors such as altimeters and magnetometers. The integration of satellite and inertial measurements, referred to as GNSS/INS integration, has been studied for several decades [1]–[3]. Typically, the integration is based on an extended Kalman filter (EKF).

Driven by advances in sensor technology, low-cost satellite receivers and inertial instruments are appearing in an increasingly wide range of products, including mobile phones, cars, and small unmanned vehicles. This development has spurred an interest in constructing observers with lower computational complexity than the EKF by using tools from nonlinear control and estimation theory. An advantage of such designs is that they often come with global or semiglobal stability proofs.

Most of the effort on navigation observers has been directed toward the problem of estimating the attitude, usually based on an explicit attitude measurement or the comparison of body-fixed vector measurements with reference vectors in a reference coordinate system [4]–[9]. A survey of attitude estimation methods is given by Crassidis, Markley, and Cheng [10]. Vik and Fossen [11] studied the GNSS/INS integration problem including attitude, position, velocity, and inertial sensor bias, with the assumption that the attitude could be measured independently from the position and velocity. Hua [12] did not make this assumption, and constructed two algorithms for estimating attitude and velocity based only on GNSS velocity together with inertial and magnetometer measurements.

The work of Håvard Fjær Grip is supported by the Research Council of Norway. The work of Ali Saberi is partially supported by NAVY grants ONR KKK777SB001 and ONR KKK760SB0012.

A. Topics of This Paper

In this paper we consider a problem similar to that of Hua [12]—specifically, the estimation of attitude, position, and velocity by integrating GNSS, inertial, and magnetometer data. Unlike Hua, however, we also consider estimation of gyro bias, which is prevalent in low-cost inertial sensors and typically included in EKF-based solutions. Moreover, we present stability results that guarantee global exponential convergence. To the authors' knowledge, the literature contains no similarly strong stability results for GNSS/INS integration with gyro bias estimation.

The attitude that we seek to estimate is represented by a rotation matrix R, which belongs to the special orthogonal group SO(3). Nevertheless, we do not restrict our estimate $\hat{R}$ to SO(3), but rather allow it to develop with nine degrees of freedom in the transient phase before it converges to R. This type of over-parameterization avoids well-known topological obstructions that prevent global results on SO(3), but it has the drawback of not guaranteeing an orthogonal attitude estimate at all times. This drawback can be addressed by post-orthogonalizing and regularizing the estimate, a strategy that is discussed, for example, by Batista, Silvestre, and Oliveira [13], [14], who considered globally exponentially stable attitude estimation using observers similar to the attitude part of our observer.

Our overall design is based on a general design methodology for interconnected nonlinear and linear systems, recently presented by the some of the authors [15], [16]. In these papers, a simplified version of the GNSS/INS integration algorithm, without gyro bias estimation, was used as an application example.

B. Notation and Preliminaries

For a vector or matrix X, X' denotes its transpose. The operator $\|\cdot\|$ denotes the Euclidean norm for vectors and the Frobenius norm for matrices. For a symmetric positive-semidefinite matrix A, the minimum eigenvalue is denoted by $\lambda_{\min}(A)$. The skew-symmetric part of a square matrix A is denoted by $\mathbb{P}_{\mathrm{a}}(A) = \frac{1}{2}(A - A')$. For a vector $x \in \mathbb{R}^3$, $S(x)$ denotes the skew-symmetric matrix

$$S(x) = \begin{bmatrix} 0 & -x_3 & x_2 \\ x_3 & 0 & -x_1 \\ -x_2 & x_1 & 0 \end{bmatrix}.$$

The linear function $\mathrm{vex}(A)$ such that $S(\mathrm{vex}(A)) = A$ and $\mathrm{vex}(S(x)) = x$ is well-defined for all 3×3 skew-symmetric matrix arguments. The function $\mathrm{sat}(\cdot)$ denotes a component-wise saturation of its vector or matrix argument to the interval $[-1, 1]$. We denote by I_n the $n \times n$ identity matrix and by $0_{m \times n}$ the $m \times n$ matrix with zero elements.

Throughout the paper, we consider all dynamical systems to be initialized at time $t = 0$. All time-varying signals are assumed to be at least piecewise continuous. We omit function arguments when possible without confusion.

II. Problem Formulation

We operate with two different coordinate frames, namely, the Earth-fixed North-East-Down frame (NED), and the body-fixed frame (BODY). The superscripts $^{\mathrm{n}}$ and $^{\mathrm{b}}$ are used to distinguish between these frames. The dynamics of the position, velocity, and attitude is described by the equations

$$\dot{p}^{\mathrm{n}} = v^{\mathrm{n}}, \tag{1a}$$

$$\dot{v}^{\mathrm{n}} = a^{\mathrm{n}} + g^{\mathrm{n}}, \tag{1b}$$

$$\dot{R} = RS(\omega^{\mathrm{b}}), \tag{1c}$$

where p^{n} and v^{n} are position and velocity vectors in NED; $R \in \mathrm{SO}(3)$ is a rotation matrix from BODY to NED; ω^{b} is the angular velocity of the BODY frame relative to the NED frame, decomposed in BODY coordinates; g^{n} is the gravity vector in NED; and a^{n} is the proper acceleration in NED.[1]

Our goal is to estimate the position p^{n}, velocity v^{n}, and attitude R with exponential convergence rate. To achieve this goal, we shall also introduce an auxiliary bias estimate.

A. Measurements

We assume that the sensor suite consists of a GNSS receiver, 6-axis inertial instruments, and a 3-axis magnetometer (or another equivalent vector measurement). These instruments provide the following information:

- measurements of the NED position p^{n} and velocity v^{n} (in Section III-D we consider the case when only p^{n} is available)
- a biased angular velocity measurement $\omega^{\mathrm{b}}_{\mathrm{m}} = \omega^{\mathrm{b}} + b$, where b represents the bias
- an acceleration measurement a^{b}, which is related to a^{n} by $a^{\mathrm{n}} = Ra^{\mathrm{b}}$
- a magnetometer measurement m^{b}, which is related to the Earth's magnetic field m^{n} at the current location by $m^{\mathrm{n}} = Rm^{\mathrm{b}}$

Although we will not perform any explicit differentiations, we assume that the derivative $\dot{a}^{\mathrm{b}}$ of the BODY acceleration is well-defined and bounded. Naturally, we can also assume that a^{b}, m^{b}, and ω^{b} are bounded, and that $\|m^{\mathrm{b}}\|$ is lower-bounded by a positive constant. We make the following assumption regarding the gyro bias.

Assumption 1: The gyro bias b is constant, and there exists a known constant $M_b > 0$ such that $\|b\| \leq M_b$.

[1] In this paper we assume that the NED frame is an inertial coordinate frame. In high-precision applications, the rotation of the Earth must also be accounted for in the kinematic equations.

We make the following standard assumption to ensure uniform observability (see, e.g., [6], [12]).

Assumption 2: There exists a constant $c_{\mathrm{obs}} > 0$ such that, for all $t \geq 0$, $\|m^{\mathrm{b}} \times a^{\mathrm{b}}\| \geq c_{\mathrm{obs}}$.

III. Observer

Our design strategy is divided into two stages. In the first stage, we construct an observer for R and b (but not p^{n} and v^{n}), which is based on comparing vector measurements in the BODY coordinate system with reference vectors in the NED coordinate system; specifically, m^{b} is compared to m^{n}, and a^{b} is compared to a^{n}. This observer is not directly implementable because a^{n} is not available as a measurement. In the second stage, we therefore recover the design using only measured signals, by constructing an observer for p^{n} and v^{n}, as well as a^{n}, that is combined with the observer designed in the first stage. This two-stage technique is based on the theory of Grip, Saberi, and Johansen on observer design for interconnected systems [15], [16].

A. Stage I: Observer for R and b

Let us consider the problem of estimating the attitude R and gyro bias b, assuming for the time being that a^{n} is available as a measurement. Since $m^{\mathrm{n}} = Rm^{\mathrm{b}}$ and $a^{\mathrm{n}} = Ra^{\mathrm{b}}$, we can base the design on comparing m^{b} with m^{n} and a^{b} with a^{n}. Specifically, we design an observer

$$\dot{\hat{R}} = \hat{R}S(\omega^{\mathrm{b}}_{\mathrm{m}} - \hat{b}) + \sigma K_P J, \tag{2a}$$

$$\dot{\hat{b}} = \mathrm{Proj}(\hat{b}, -k_I \,\mathrm{vex}(\mathbb{P}_{\mathrm{a}}(\hat{R}_{\mathrm{s}}' K_P J))). \tag{2b}$$

where $\hat{R}_{\mathrm{s}} = \mathrm{sat}(\hat{R})$. In the observer (2), J is a stabilizing output injection term inspired by the TRIAD algorithm [17], defined as

$$J(a^{\mathrm{b}}, a^{\mathrm{n}}, m^{\mathrm{b}}, m^{\mathrm{n}}, \hat{R}) = A_{\mathrm{n}} A_{\mathrm{b}}' - \hat{R} A_{\mathrm{b}} A_{\mathrm{b}}', \tag{3a}$$

$$A_{\mathrm{b}} = \begin{bmatrix} m^{\mathrm{b}} & m^{\mathrm{b}} \times a^{\mathrm{b}} & m^{\mathrm{b}} \times (m^{\mathrm{b}} \times a^{\mathrm{b}}) \end{bmatrix}, \tag{3b}$$

$$A_{\mathrm{n}} = \begin{bmatrix} m^{\mathrm{n}} & m^{\mathrm{n}} \times a^{\mathrm{n}} & m^{\mathrm{n}} \times (m^{\mathrm{n}} \times a^{\mathrm{n}}) \end{bmatrix}. \tag{3c}$$

The matrix K_P is a symmetric positive-definite gain matrix, and k_I is a positive scalar gain. The scalar $\sigma \geq 1$ is a scaling factor that will be tuned in order to achieve stability. Finally, $\mathrm{Proj}(\cdot, \cdot)$ denotes a parameter projection [18, App. E], which ensures that $\|\hat{b}\|$ remains smaller than some design constant $M_{\hat{b}} > M_b$. The details of the parameter projection are given in the Appendix.

Defining the estimation errors $\tilde{R} = R - \hat{R}$ and $\tilde{b} = b - \hat{b}$, we obtain the error dynamics

$$\dot{\tilde{R}} = RS(\omega^{\mathrm{b}}) - \hat{R}S(\omega^{\mathrm{b}}_{\mathrm{m}} - \hat{b}) - \sigma K_P J, \tag{4a}$$

$$\dot{\tilde{b}} = -\mathrm{Proj}(\hat{b}, -k_I \,\mathrm{vex}(\mathbb{P}_{\mathrm{a}}(\hat{R}_{\mathrm{s}}' K_P J))), \tag{4b}$$

which satisfies the following preliminary lemma.

Lemma 1: For any given choice of K_P and k_I, there exists a $\sigma^* \geq 1$ such that, for all $\sigma \geq \sigma^*$, the origin of the error dynamics (4) is exponentially stable with all initial conditions satisfying $\|\hat{b}(0)\| \leq M_{\hat{b}}$ contained in the region of attraction.

Proof: Noting that

$$RS(\omega^{\mathrm{b}}) - \hat{R}S(\omega^{\mathrm{b}}_{\mathrm{m}} - \hat{b}) = \tilde{R}S(\omega^{\mathrm{b}}) - RS(\tilde{b}) + \tilde{R}S(\tilde{b}),$$

we can rewrite the error dynamics as

$$\dot{\tilde{R}} = \tilde{R}S(\omega^{\mathrm{b}} + \tilde{b}) - RS(\tilde{b}) - \sigma K_P J, \tag{5a}$$

$$\dot{\hat{b}} = -\operatorname{Proj}(\hat{b}, -k_I \operatorname{vex}(\mathbb{P}_{\mathrm{a}}(\hat{R}_{\mathrm{s}}' K_P J))), \tag{5b}$$

which is locally Lipschitz, uniformly in time (see Lemma 3 in the Appendix regarding the projection). Define the function $P = \frac{1}{2}\|\hat{b}\|^2$. The derivative along the trajectories of the system is $\dot{P} = \hat{b}' \operatorname{Proj}(\hat{b}, -k_I \operatorname{vex}(\mathbb{P}_{\mathrm{a}}(\hat{R}_{\mathrm{s}}' K_P J)))$, for which we have that $\|\hat{b}\| \geq M_{\hat{b}} \implies \dot{P} \leq 0$ (see Lemma 3 in the Appendix). Hence, $\|\hat{b}\|$ cannot escape the region defined by $\|\hat{b}\| \leq M_{\hat{b}}$ for any solution of the system. We shall study the trajectories of the function

$$V(t, \tilde{R}, \tilde{b}) = \frac{1}{2}\|\tilde{R}\|^2 - \ell \operatorname{tr}(S(\tilde{b})R'\tilde{R}) + \frac{\ell\sigma}{k_I}\|\tilde{b}\|^2,$$

where $0 < \ell \leq 1$ is yet to be determined, using the knowledge that $\|\hat{b}\| \leq M_{\hat{b}}$, which implies $\|\tilde{b}\| \leq M_{\tilde{b}} := M_b + M_{\hat{b}}$. Using the properties that (for arbitrary $X \in \mathbb{R}^{3\times 3}$ and $x \in \mathbb{R}^3$) $|\operatorname{tr}(X)| \leq \sqrt{3}\|X\|$, $\|RX\| = \|X\|$, and $\|S(x)\| = \sqrt{2}\|x\|$, we have

$$V \geq \frac{1}{2}\|\tilde{R}\|^2 - \ell\sqrt{6}\|\tilde{b}\|\|\tilde{R}\| + \frac{\ell}{k_I}\|\tilde{b}\|^2,$$

and hence V is positive definite if $\ell < 1/(3k_I)$. It follows that there are positive constants α_1 and α_2 such that $\alpha_1(\|\tilde{R}\|^2 + \|\tilde{b}\|^2) \leq V \leq \alpha_2(\|\tilde{R}\|^2 + \|\tilde{b}\|^2)$. The derivative of V along the trajectories of (5) satisfies

$$\begin{aligned}
\dot{V} &= \operatorname{tr}(\tilde{R}'\dot{\tilde{R}}) - \ell \operatorname{tr}(S(\dot{\tilde{b}})R'\tilde{R}) - \ell \operatorname{tr}(S(\tilde{b})\dot{R}'\tilde{R}) \\
&\quad - \ell \operatorname{tr}(S(\tilde{b})R'\dot{\tilde{R}}) + \frac{2\ell\sigma}{k_I}\tilde{b}'\dot{\tilde{b}} \\
&= \operatorname{tr}(\tilde{R}'(\tilde{R}S(\omega^{\mathrm{b}} + \tilde{b}) - RS(\tilde{b}))) - \sigma \operatorname{tr}(\tilde{R}'K_P J) \\
&\quad + \ell \operatorname{tr}(S(\operatorname{Proj}(\hat{b}, -k_I \operatorname{vex}(\mathbb{P}_{\mathrm{a}}(\hat{R}_{\mathrm{s}}' K_P J))))R'\tilde{R}) \\
&\quad - \ell \operatorname{tr}(S(\tilde{b})S'(\omega^{\mathrm{b}})R'\tilde{R}) \\
&\quad - \ell \operatorname{tr}(S(\tilde{b})R'\tilde{R}S(\omega^{\mathrm{b}} + \tilde{b})) \\
&\quad + \ell \operatorname{tr}(S(\tilde{b})R'RS(\tilde{b})) + \ell\sigma \operatorname{tr}(S(\tilde{b})R'K_P J) \\
&\quad - \frac{2\ell\sigma}{k_I}\tilde{b}' \operatorname{Proj}(\hat{b}, -k_I \operatorname{vex}(\mathbb{P}_{\mathrm{a}}(\hat{R}_{\mathrm{s}}' K_P J))).
\end{aligned}$$

We consider the terms above more closely, starting with the second term. Since $A_{\mathrm{n}} = RA_{\mathrm{b}}$, we can write $J = \tilde{R}A_{\mathrm{b}}A_{\mathrm{b}}'$. We then have $\operatorname{tr}(\tilde{R}'K_P J) = \operatorname{tr}(\tilde{R}'K_P\tilde{R}A_{\mathrm{b}}A_{\mathrm{b}}') \geq \lambda_{\min}(A_{\mathrm{b}}A_{\mathrm{b}}')\operatorname{tr}(\tilde{R}'K_P\tilde{R}) = \lambda_{\min}(A_{\mathrm{b}}A_{\mathrm{b}}')\operatorname{tr}(\tilde{R}\tilde{R}'K_P) \geq \lambda_{\min}(A_{\mathrm{b}}A_{\mathrm{b}}')\lambda_{\min}(K_P)\|\tilde{R}\|^2$ (see, e.g., [19]). Using Assumption 2 it can be shown that there is a $c > 0$ such that $\lambda_{\min}(A_{\mathrm{b}}A_{\mathrm{b}}') \geq c^2$ (see [15], [16]). Hence, $\operatorname{tr}(\tilde{R}'K_P J) \geq \lambda_{\min}(K_P)c^2\|\tilde{R}\|^2$.

Using the property that $\operatorname{tr}(\tilde{R}'\tilde{R}S(x)) = 0$ (due to symmetry of $\tilde{R}'\tilde{R}$; see, e.g., [6]), we can bound the first term by $\sqrt{6}\|\tilde{R}\|\|\tilde{b}\|$. Similarly, we can bound the fourth term by $2\sqrt{3}\ell M_\omega\|\tilde{R}\|\|\tilde{b}\|$, where M_ω is a bound on $\|\omega^{\mathrm{b}}\|$, and the fifth term by $2\sqrt{3}\ell(M_\omega + M_{\tilde{b}})\|\tilde{R}\|\|\tilde{b}\|$. Using the additional properties that $\|\operatorname{Proj}(\hat{b}, x)\| \leq \|x\|$ (Lemma 3 in the Appendix), $\|\operatorname{vex}(\mathbb{P}_{\mathrm{a}}(X))\| \leq \frac{1}{\sqrt{2}}\|X\|$, $\|\hat{R}_{\mathrm{s}}\| \leq 3$, and $\|J\| = \|\tilde{R}A_{\mathrm{b}}A_{\mathrm{b}}'\| \leq \|\tilde{R}\|\|A_{\mathrm{b}}\|^2$, we can bound the third term by $3\sqrt{3}\ell k_I\|K_P\|M_A^2\|\tilde{R}\|^2$, where M_A is a bound on $\|A_{\mathrm{b}}\|$.

For the sixth term, we have that $\operatorname{tr}(S(\tilde{b})R'RS(\tilde{b})) = -\operatorname{tr}(S'(\tilde{b})S(\tilde{b})) = -2\|\tilde{b}\|^2$, where we have used the property that $\operatorname{tr}(S'(x)S(y)) = 2x'y$ (e.g., [6]). For the eight term, we have that $-\tilde{b}'\operatorname{Proj}(\hat{b}, -k_I \operatorname{vex}(\mathbb{P}_{\mathrm{a}}(\hat{R}_{\mathrm{s}}' K_P J))) \leq k_I\tilde{b}' \operatorname{vex}(\mathbb{P}_{\mathrm{a}}(\hat{R}_{\mathrm{s}}' K_P J)) = \frac{1}{2}k_I \operatorname{tr}(S'(\tilde{b})\mathbb{P}_{\mathrm{a}}(\hat{R}_{\mathrm{s}}' K_P J)) = \frac{1}{2}k_I \operatorname{tr}(S'(\tilde{b})\hat{R}_{\mathrm{s}}' K_P J) = -\frac{1}{2}k_I \operatorname{tr}(S(\tilde{b})\hat{R}_{\mathrm{s}}' K_P J)$, where we have used the properties that $-\tilde{b}'\operatorname{Proj}(\hat{b}, x) \leq -\tilde{b}'x$ (Lemma 3 of the Appendix) and $\operatorname{tr}(S(x)X) = \operatorname{tr}(S(x)\mathbb{P}_{\mathrm{a}}(X))$ (e.g., [6]). Considering the seventh and eight term together, and using the fact that $\|R - \hat{R}_{\mathrm{s}}\| \leq \|\tilde{R}\|$ we therefore have $\ell\sigma \operatorname{tr}(S(\tilde{b})R'K_P J) - 2\ell\sigma/k_I\tilde{b}'\operatorname{Proj}(\hat{b}, -k_I \operatorname{vex}(\mathbb{P}_{\mathrm{a}}(\hat{R}_{\mathrm{s}}' K_P J))) \leq \ell\sigma \operatorname{tr}(S(\tilde{b})R'K_P J) - \ell\sigma \operatorname{tr}(S(\tilde{b})\hat{R}_{\mathrm{s}}' K_P J) \leq \sqrt{6}\ell\sigma\|K_P\|M_{\tilde{b}}M_A^2\|\tilde{R}\|^2$.

Taking all these inequalities together, we can write

$$\begin{aligned}
\dot{V} &\leq -\sigma\lambda_{\min}(K_P)c^2\|\tilde{R}\|^2 + \sqrt{6}\|\tilde{R}\|\|\tilde{b}\| \\
&\quad + 2\sqrt{3}\ell M_\omega\|\tilde{R}\|\|\tilde{b}\| + 2\sqrt{3}\ell(M_\omega + M_{\tilde{b}})\|\tilde{R}\|\|\tilde{b}\| \\
&\quad + 3\sqrt{3}\ell k_I\|K_P\|M_A^2\|\tilde{R}\|^2 - 2\ell\|\tilde{b}\|^2 \\
&\quad + \sqrt{6}\ell\sigma\|K_P\|M_{\tilde{b}}M_A^2\|\tilde{R}\|^2 \\
&= -\begin{bmatrix}\|\tilde{R}\| \\ \|\tilde{b}\|\end{bmatrix}' \begin{bmatrix}\sigma q_1 - \ell q_2 - \ell\sigma q_3 & -q_4 - \ell q_5 \\ -q_4 - \ell q_5 & 2\ell\end{bmatrix} \begin{bmatrix}\|\tilde{R}\| \\ \|\tilde{b}\|\end{bmatrix},
\end{aligned}$$

for some constants $q_1, \dots, q_5$ that are independent of ℓ and σ. Let ℓ be sufficiently small that $q_1 - \ell q_3 \geq r_1$ for some $r_1 > 0$, and note that ℓ is chosen independently from σ. Then

$$\dot{V} \leq -\begin{bmatrix}\|\tilde{R}\| \\ \|\tilde{b}\|\end{bmatrix}' \begin{bmatrix}\sigma r_1 - \ell q_2 & -q_4 - \ell q_5 \\ -q_4 - \ell q_5 & 2\ell\end{bmatrix} \begin{bmatrix}\|\tilde{R}\| \\ \|\tilde{b}\|\end{bmatrix}.$$

The first-order principal minor of the above matrix is positive if σ is chosen large enough that $\sigma > \ell q_2/r_1$. The second-order principal minor is positive if σ is chosen large enough that $\sigma > ((q_4 + \ell q_5)^2 + 2\ell^2 q_2)/(2\ell r_1)$. Hence, for sufficiently large σ, there exists an $\alpha_3 > 0$ such that $\dot{V} \leq -\alpha_3(\|\tilde{R}\|^2 + \|\tilde{b}\|^2)$. By invoking the comparison lemma [20, Lemma 3.4], the exponential stability result follows. ■

B. Stage II: Recovery Using Measured Signals

As discussed above, the observer (2) cannot be directly implemented, because it depends on the unmeasured variable a^{n}. However, according to (1a) and (1b), a^{n} can be viewed as an input to a linear system with states v^{n} and p^{n}, from which the outputs p^{n} and v^{n} are available. This results in a cascaded system structure, illustrated in Fig. 1, that has previously been studied by Grip et al. in a general context [15], [16]. Following the design methodology of Grip et al., we obtain an observer for p^{n} and v^{n}, as well as the NED acceleration a^{n}, given by

$$\dot{\hat{p}}^{\mathrm{n}} = \hat{v}^{\mathrm{n}} + K_{pp}(p^{\mathrm{n}} - \hat{p}^{\mathrm{n}}) + K_{pv}(v^{\mathrm{n}} - \hat{v}^{\mathrm{n}}), \tag{6a}$$

$$\dot{\hat{v}}^{\mathrm{n}} = \hat{a}^{\mathrm{n}} + g^{\mathrm{n}} + K_{vp}(p^{\mathrm{n}} - \hat{p}^{\mathrm{n}}) + K_{vv}(v^{\mathrm{n}} - \hat{v}^{\mathrm{n}}), \tag{6b}$$

$$\dot{\xi} = -\sigma K_P \hat{J} a^{\mathrm{b}} + K_{\xi p}(p^{\mathrm{n}} - \hat{p}^{\mathrm{n}}) + K_{\xi v}(v^{\mathrm{n}} - \hat{v}^{\mathrm{n}}), \tag{6c}$$

$$\hat{a}^{\mathrm{n}} = \hat{R}a^{\mathrm{b}} + \xi, \tag{6d}$$

where $\hat{J} = J(a^{\mathrm{b}}, \hat{a}^{\mathrm{n}}, m^{\mathrm{b}}, m^{\mathrm{n}}, \hat{R})$, and where K_{pp}, K_{pv}, K_{vp}, K_{vv}, $K_{\xi p}$, and $K_{\xi v}$ are observer gains yet to be determined. The

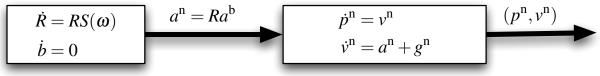

Fig. 1. Illustration of system structure

observer (2) is implemented with J replaced by $\hat{J}$:

$$\dot{\hat{R}} = \hat{R}S(\omega_{\mathrm{m}}^{\mathrm{b}} - \hat{b}) + \sigma K_P \hat{J}, \tag{7a}$$

$$\dot{\hat{b}} = \mathrm{Proj}(\hat{b}, -k_I \,\mathrm{vex}(\mathbb{P}_{\mathrm{a}}(\hat{R}_{\mathrm{s}}' K_P \hat{J}))). \tag{7b}$$

The observer (6), (7) depends only on known quantities.

C. Main Result

In this section we present our main stability result for the observer (6), (7). Defining the error variables $\tilde{p}^{\mathrm{n}} = p^{\mathrm{n}} - \hat{p}^{\mathrm{n}}$ and $\tilde{v}^{\mathrm{n}} = v^{\mathrm{n}} - \hat{v}^{\mathrm{n}}$, we obtain the error dynamics

$$\dot{\tilde{p}}^{\mathrm{n}} = \tilde{v}^{\mathrm{n}} - K_{pp}\tilde{p}^{\mathrm{n}} - K_{pv}\tilde{v}^{\mathrm{n}}, \tag{8a}$$

$$\dot{\tilde{v}}^{\mathrm{n}} = \tilde{a}^{\mathrm{n}} - K_{vp}\tilde{p}^{\mathrm{n}} - K_{vv}\tilde{v}^{\mathrm{n}}, \tag{8b}$$

where $\tilde{a}^{\mathrm{n}} = a^{\mathrm{n}} - \hat{a}^{\mathrm{n}}$. To find the dynamics of $\tilde{a}^{\mathrm{n}}$, we note that $\dot{a}^{\mathrm{n}} = \dot{R}a^{\mathrm{b}} + R\dot{a}^{\mathrm{b}} = RS(\omega^{\mathrm{b}})a^{\mathrm{b}} + R\dot{a}^{\mathrm{b}}$ and that

$$\begin{aligned}\dot{\hat{a}}^{\mathrm{n}} &= \dot{\hat{R}}a^{\mathrm{b}} + \hat{R}\dot{a}^{\mathrm{b}} + \dot{\xi} \\ &= (\hat{R}S(\omega_{\mathrm{m}}^{\mathrm{b}} - \hat{b}) + \sigma K_P \hat{J})a^{\mathrm{b}} + \hat{R}\dot{a}^{\mathrm{b}} \\ &\quad - \sigma K_P \hat{J} a^{\mathrm{b}} + K_{\xi p}(p^{\mathrm{n}} - \hat{p}^{\mathrm{n}}) + K_{\xi v}(v^{\mathrm{n}} - \hat{v}^{\mathrm{n}}) \\ &= \hat{R}S(\omega_{\mathrm{m}}^{\mathrm{b}} - \hat{b})a^{\mathrm{b}} + \hat{R}\dot{a}^{\mathrm{b}} + K_{\xi p}(p^{\mathrm{n}} - \hat{p}^{\mathrm{n}}) + K_{\xi v}(v^{\mathrm{n}} - \hat{v}^{\mathrm{n}}).\end{aligned}$$

Hence,

$$\dot{\tilde{a}}^{\mathrm{n}} = -K_{\xi p}\tilde{p}^{\mathrm{n}} - K_{\xi v}\tilde{v}^{\mathrm{n}} + \tilde{d}, \tag{9}$$

where $\tilde{d} = (RS(\omega^{\mathrm{b}}) - \hat{R}S(\omega_{\mathrm{m}}^{\mathrm{b}} - \hat{b}))a^{\mathrm{b}} + (R - \hat{R})\dot{a}^{\mathrm{b}}$. Defining the error variable $\tilde{w} = [(\tilde{p}^{\mathrm{n}})', (\tilde{v}^{\mathrm{n}})', (\tilde{a}^{\mathrm{n}})']'$, we can write the error dynamics (8), (9) more compactly as

$$\dot{\tilde{w}} = (A - KC)\tilde{w} + B\tilde{d}, \tag{10}$$

where

$$A = \begin{bmatrix} 0_{6\times 3} & I_6 \\ 0_{3\times 3} & 0_{3\times 6} \end{bmatrix}, \quad B = \begin{bmatrix} 0_{6\times 3} \\ I_3 \end{bmatrix},$$

$$C = \begin{bmatrix} I_6 & 0_{6\times 3} \end{bmatrix}, \quad K = \begin{bmatrix} K_{pp} & K_{pv} \\ K_{vp} & K_{vv} \\ K_{\xi p} & K_{\xi v} \end{bmatrix}.$$

The dynamics of the errors $\tilde{R}$ and $\tilde{b}$ becomes the same as (4), with J replaced by $\hat{J}$:

$$\dot{\tilde{R}} = RS(\omega^{\mathrm{b}}) - \hat{R}S(\omega_{\mathrm{m}}^{\mathrm{b}} - \hat{b}) - \sigma K_P \hat{J}, \tag{11a}$$

$$\dot{\tilde{b}} = -\mathrm{Proj}(\hat{b}, -k_I \,\mathrm{vex}(\mathbb{P}_{\mathrm{a}}(\hat{R}_{\mathrm{s}}' K_P \hat{J}))). \tag{11b}$$

The following theorem shows that by properly selecting the gain matrix K, the origin of the error dynamics can be rendered exponentially stable.

Lemma 2: Let σ be chosen to ensure stability according to Lemma 1 and define $H_K(s) = (Is - A + KC)^{-1}B$. There exists a $\gamma > 0$ such that, if the gain matrix K is chosen such that $A - KC$ is Hurwitz and $\|H_K(s)\|_\infty < \gamma$, then the origin of the error dynamics (10), (11) is exponentially stable with all initial conditions satisfying $\|\hat{b}(0)\| \le M_{\hat{b}}$ contained in the region of attraction. Moreover, K can always be chosen to satisfy these conditions.

Proof: It is straightforward to verify that the pair (A, C) is observable and that the triple (A, B, C) is left-invertible and minimum-phase. It therefore follows from Theorem 2 of Grip et al. [16] that K can always be chosen to satisfy the requirements of Lemma 2. As in the proof of Lemma 1, we know that the solutions cannot escape the region defined by $\|\hat{b}\| \le M_{\hat{b}}$.

The error dynamics (11) can be written as

$$\begin{aligned}\dot{\tilde{R}} &= RS(\omega^{\mathrm{b}}) - \hat{R}S(\omega_{\mathrm{m}}^{\mathrm{b}} - \hat{b}) - \sigma K_P J + \sigma K_P \tilde{J}, \\ \dot{\tilde{b}} &= -\mathrm{Proj}(\hat{b}, \tau(J)) + \mathrm{Proj}(\hat{b}, \tau(J)) - \mathrm{Proj}(\hat{b}, \tau(\hat{J})),\end{aligned}$$

where $\tilde{J} = J - \hat{J}$ and $\tau(J) = -k_I \,\mathrm{vex}(\mathbb{P}_{\mathrm{a}}(\hat{R}_{\mathrm{s}}' K_P J))$. We can write $\tilde{J} = (A_{\mathrm{n}} - \hat{A}_{\mathrm{n}})A_{\mathrm{b}}'$, where $\hat{A}_{\mathrm{n}}$ is defined like A_{n} with a^{n} replaced by $\hat{a}^{\mathrm{n}}$. Since A_{n} is linear in a^{n} and A_{b} is bounded, it follows that $\|\sigma K_P \tilde{J}\| \le s_1 \|\tilde{a}^{\mathrm{n}}\|$ for some $s_1 > 0$. Using the techniques of the proof of Lemma 1, we can easily show that there is an $s_2 > 0$ such that $\|\tau(J) - \tau(\hat{J})\| \le s_2 \|\tilde{a}^{\mathrm{n}}\|$. It can therefore be verified that $\|\mathrm{Proj}(\hat{b}, \tau(J)) - \mathrm{Proj}(\hat{b}, \tau(\hat{J}))\| \le s_3 \|\tilde{a}^{\mathrm{n}}\|$ for some $s_3 > 0$. Considering again the function V from the proof of Lemma 1, we therefore have

$$\begin{aligned}\dot{V} &\le -\alpha_3(\|\tilde{R}\|^2 + \|\tilde{b}\|^2) + \mathrm{tr}(\tilde{R}'\sigma K_P \tilde{J}) \\ &\quad - \ell\,\mathrm{tr}(S(\mathrm{Proj}(\hat{b}, \tau(J)) - \mathrm{Proj}(\hat{b}, \tau(\hat{J})))R'\tilde{R}) \\ &\quad - \ell\,\mathrm{tr}(S(\tilde{b})R'\sigma K_P \tilde{J}) \\ &\quad + \frac{2\sigma\ell}{k_I}\tilde{b}'(\mathrm{Proj}(\hat{b}, \tau(J)) - \mathrm{Proj}(\hat{b}, \tau(\hat{J}))) \\ &\le -\alpha_3(\|\tilde{R}\|^2 + \|\tilde{b}\|^2) + \sqrt{3}s_1\|\tilde{R}\|\|\tilde{a}^{\mathrm{n}}\| \\ &\quad + \sqrt{6}\ell s_3\|\tilde{R}\|\|\tilde{a}^{\mathrm{n}}\| + \sqrt{6}\ell s_1\|\tilde{b}\|\|\tilde{a}^{\mathrm{n}}\| + \frac{2\sigma\ell s_3}{k_I}\|\tilde{b}\|\|\tilde{a}^{\mathrm{n}}\| \\ &\le -\alpha_3\zeta^2 + p_1\zeta\|\tilde{w}\|,\end{aligned}$$

for some $p_1 > 0$, where $\zeta := (\|\tilde{R}\|^2 + \|\tilde{b}\|^2)^{1/2}$.

Next, from following the proof Theorem 1 of Grip et al. [16], there is a function $W = \tilde{w}'P\tilde{w}$, for some positive-definite matrix P, such that $\dot{W} \le -\|\tilde{w}\|^2 + \gamma^2\|\tilde{d}\|^2$. Using the expression at the beginning of the proof of Lemma 1, we can rewrite $\tilde{d}$ as $(\tilde{R}S(\omega^{\mathrm{b}}) - RS(\tilde{b}) + \tilde{R}S(\tilde{b}))a^{\mathrm{b}} + \tilde{R}\dot{a}^{\mathrm{b}}$, which is bounded by $\sqrt{2}(M_\omega M_a\|\tilde{R}\| + M_a\|\tilde{b}\| + M_{\tilde{b}}M_a\|\tilde{R}\|) + M_{\dot{a}}\|\tilde{R}\|$, where M_a and $M_{\dot{a}}$ are bounds on $\|a^{\mathrm{b}}\|$ and $\dot{a}^{\mathrm{b}}$. Hence, $\dot{W} \le -\|\tilde{w}\|^2 + \gamma^2 p_2^2 \zeta^2$ for some $p_2 > 0$.

Consider now the function $U = W + \gamma V$, for which we have

$$\dot{U} \le -\begin{bmatrix} \|\tilde{w}\| & \zeta \end{bmatrix} \begin{bmatrix} 1 & -\frac{1}{2}\gamma p_1 \\ -\frac{1}{2}\gamma p_1 & \gamma\alpha_3 - \gamma^2 p_2^2 \end{bmatrix} \begin{bmatrix} \|\tilde{w}\| \\ \zeta \end{bmatrix}.$$

The first-order principal minor of the above matrix is positive, and the second-order principal minor is positive if $\gamma < 4\alpha_3/(p_1^2 + 4p_2^2)$. By invoking the comparison lemma [20, Lemma 3.4], we obtain the desired stability result. ■

The result of Lemma 2 is, for all practical purposes, a global exponential stability result. The only restriction on the initial conditions is that $\|\hat{b}(0)\| \le M_{\hat{b}}$. Any choice of initial conditions that does not satisfy this restriction is meaningless, since the actual bias b is known to satisfy $\|b\| \le M_b < M_{\hat{b}}$. Nevertheless, in order to state a formal result of exponential convergence from arbitrary initial conditions, we introduce the following resetting rule:

If at any time $t \ge 0$, $\|\hat{b}(t)\| > M_{\hat{b}}$, then $\hat{b}$ is reset to

$$b(t^+) = M_{\hat{b}} \frac{\hat{b}(t)}{\|\hat{b}(t)\|}. \tag{12}$$

The following result then follows immediately.

Theorem 1: Let σ be chosen to ensure stability according to Lemma 1. There exists a $\gamma > 0$ such that, if the gain matrix K is chosen such that $A - KC$ is Hurwitz and $\|H_K(s)\|_\infty < \gamma$, then the origin of the error dynamics (10), (11) with resetting is globally exponentially stable. Moreover, K can always be chosen to satisfy these conditions.

D. No Velocity Measurement

So far we have assumed that the GNSS receiver provides measurements of both position and velocity. Depending on the receiver, however, a high-quality velocity measurement may not be available. The lack of a velocity measurement v^n implies that we cannot use terms of the form $v^n - \hat{v}^n$ in (6). Calculating the error dynamics in this case, we find that it is still given by (10), (11), but with the matrices C and K replaced by $\bar{C} := [I_3, 0_{3\times 6}]$ and $\bar{K} := [K'_{pp}, K'_{vp}, K'_{\xi p}]'$. We can state an equally strong result for this case, which follows verbatim from the proof of Lemma 2 with C and K replaced by $\bar{C}$ and $\bar{K}$.

Theorem 2: Let σ be chosen to ensure stability according to Lemma 1 and define $\bar{H}_{\bar{K}}(s) = (Is - A + \bar{K}\bar{C})^{-1}B$. There exists a $\gamma > 0$ such that, if the gain matrix $\bar{K}$ is chosen such that $A - \bar{K}\bar{C}$ is Hurwitz and $\|\bar{H}_{\bar{K}}(s)\|_\infty < \gamma$, then the origin of the error dynamics (10), (11) with resetting is globally exponentially stable. Moreover, $\bar{K}$ can always be chosen to satisfy these conditions.

IV. Gain Selection and Tuning

According to above results, the different parts of the observer can be tuned sequentially, by first choosing K_P, k_I, and σ according to Lemma 1 and then choosing K (or $\bar{K}$) to ensure stability of the overall error dynamics.

The requirements of Lemma 1 can be met by choosing arbitrary gains K_P and k_I and gradually increasing σ until stability is achieved. In practice, K_P, k_I, and σ should be chosen through careful tuning; for example, by the use of simulations. The parameter σ can be absorbed in K_P, which can in turn be chosen as a diagonal matrix. In this case, one is left with four tuning parameters. The gain matrix K (or $\bar{K}$) can be chosen using any preferred gain selection technique, as long as one is able to reduce the $\mathscr{H}_\infty$ norm of $H_K(s)$ (or $\bar{H}_{\bar{K}}(s)$) as necessary to achieve stability. One particular possibility is to use LMIs, which allows for easy incorporation of additional performance requirements while bounding the $\mathscr{H}_\infty$ norm as desired [21], [22]. Additional discussion of gain selection using LMIs is given by Grip et al. [15], [16].

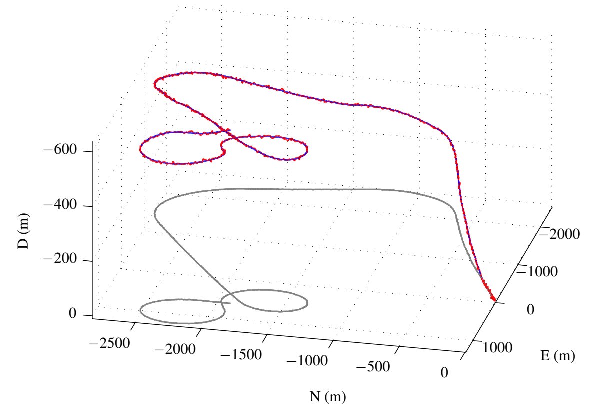

Fig. 2. True (blue, dashed) and estimated (red, solid) position in local North-East-Down coordinates (ground track at zero altitude shown in gray)

V. Simulation

The design is verified by simulating a takeoff, climb and two steep turns in a Cessna 172, using the flight simulator *X-Plane*®. Inertial measurements are available at a rate of 100 Hz, and GNSS position and velocity measurements are available at 5 Hz. Noise is added to all the measurements.

The attitude and gyro bias observer is tuned with the gains $K_P = \text{diag}(10, 0.1, 0.1)$, $k_I = 0.02$, and $\sigma = 1$. We assume that the gyro bias is limited by $\|b\| \le M_b = 2°/\text{s}$, and use $M_{\hat{b}} = 2.1°/\text{s}$ for the projection. With the help of an LMI formulation that allows $\|H_K(s)\|_\infty$ to be reduced as necessary, we choose $K_{pp} \approx 128.9I$, $K_{pv} \approx 17.5I$, $K_{vp} \approx 15.7I$, $K_{vv} \approx 2.4I$, $K_{\xi p} \approx 1.3I$, and $K_{\xi v} \approx 0.2I$.

Applying the resulting observer to the simulated measurement data, we obtain the results shown in Figs. 2–5. The estimated Euler angles shown in Fig. 4 are derived from $\hat{R}$ by inverse trigonometry.

VI. Concluding Remarks

Although the design presented in this paper has been verified using realistic flight simulation, many potential error sources (such as accelerometer bias, magnetic disturbances, GNSS failure, and mounting errors) are not included in the simulation. The focus of current research is on effectively handling such errors, and on evaluating and expanding the design based on actual flight tests.

References

[1] P. S. Maybeck, *Stochastic Models, Estimation, and Control, Volume 1*, ser. Mathematics in Science and Engineering. New York: Academic Press, 1979, vol. 141.

[2] R. Phillips and G. Schmidt, "GPS/INS integration," *AGARD Lecture Series: System Implications and Innovative Applications of Satellite Navigation*, vol. 207, pp. 9.1–9.18, 1996.

[3] M. S. Grewal, L. R. Weill, and A. P. Andrews, *Global Positioning Systems, Inertial Navigation, and Integration*. New York: Wiley, 2001.

[4] S. Salcudean, "A globally convergent angular velocity observer for rigid body motion," *IEEE Trans. Automat. Contr.*, vol. 36, no. 12, pp. 1493–1497, 1991.

[5] J. Thienel and R. M. Sanner, "A coupled nonlinear spacecraft attitude controller and observer with an unknown constant gyro bias and gyro noise," *IEEE Trans. Automat. Contr.*, vol. 48, no. 11, pp. 2011–2015, 2003.

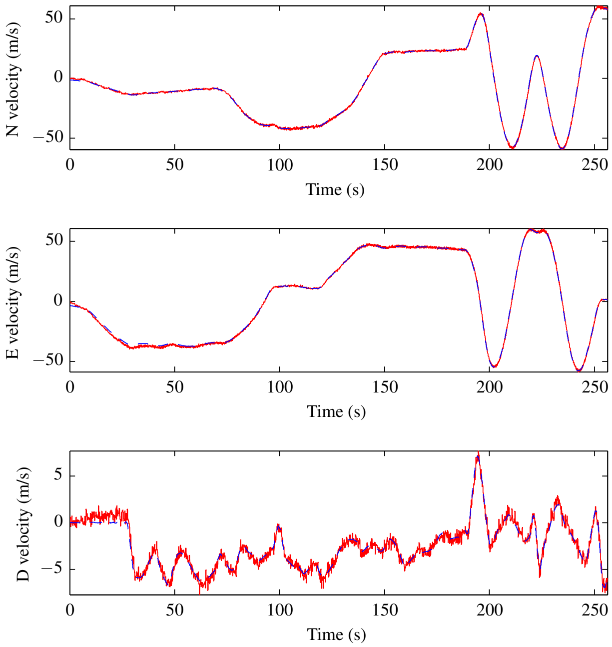

Fig. 3. True (blue, dashed) and estimated (red, solid) velocity in local North-East-Down coordinates

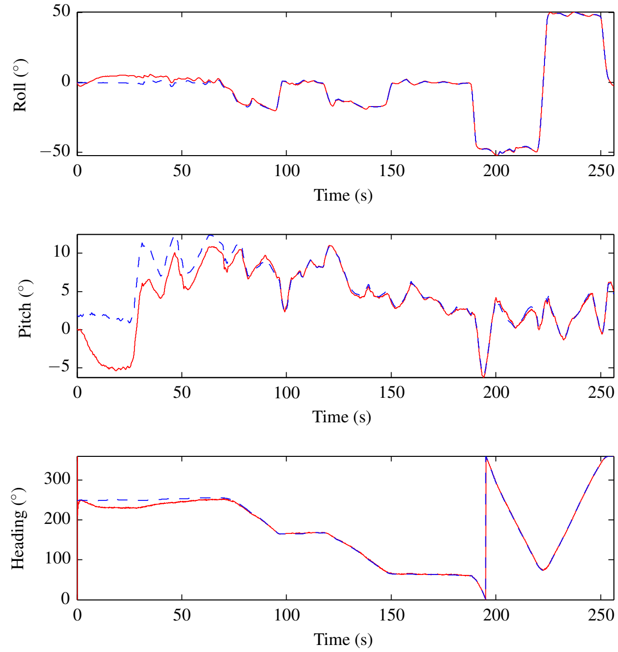

Fig. 4. True (blue, dashed) and estimated (red, solid) Euler angles

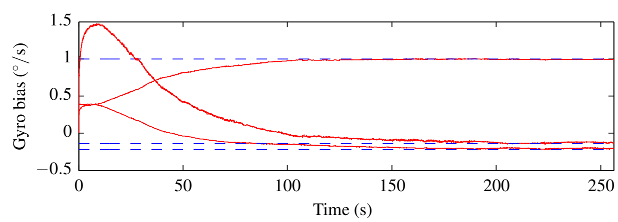

Fig. 5. True (blue, dashed) and estimated (red, solid) gyro bias

[6] R. Mahony, T. Hamel, and J.-M. Pflimlin, "Nonlinear complementary filters on the Special Orthogonal Group," *IEEE Trans. Automat. Contr.*, vol. 53, no. 5, pp. 1203–1218, 2008.
[7] R. Mahony, T. Hamel, J. Trumpf, and C. Lageman, "Nonlinear observers on SO(3) for complementary and compatible measurements: A theoretical study," in *Proc. IEEE Conf. Dec. Contr./Chinese Contr. Conf.*, Shanghai, China, 2009, pp. 6407–6412.
[8] H. F. Grip, T. I. Fossen, T. A. Johansen, and A. Saberi, "Attitude estimation based on time-varying reference vectors with biased gyro and vector measurements," in *Proc. IFAC World Congr.*, Milan, Italy, 2011, pp. 8497–8502.
[9] ——, "Attitude estimation using biased gyro and vector measurements with time-varying reference vectors," *IEEE Trans. Automat. Contr.*, 2012, to appear.
[10] J. L. Crassidis, F. L. Markley, and Y. Cheng, "Survey of nonlinear attitude estimation methods," *J. Guid. Contr. Dynam.*, vol. 30, no. 1, pp. 12–28, 2007.
[11] B. Vik and T. I. Fossen, "A nonlinear observer for GPS and INS integration," in *Proc. IEEE Conf. Dec. Contr.*, Orlando, FL, 2001, pp. 2956–2961.
[12] M.-D. Hua, "Attitude estimation for accelerated vehicles using GPS/INS measurements," *Contr. Eng. Pract.*, vol. 18, no. 7, pp. 723–732, 2010.
[13] P. Batista, C. Silvestre, and P. J. Oliveira, "GES attitude observers – Part I: Multiple general vector observations," in *Proc. IFAC World Congr.*, Milan, Italy, 2011, pp. 2985–2990.
[14] ——, "GES attitude observers – Part II: Single vector observations," in *Proc. IFAC World Congr.*, Milan, Italy, 2011, pp. 2991–2996.
[15] H. F. Grip, A. Saberi, and T. A. Johansen, "Observers for cascaded nonlinear and linear systems," in *Proc. IEEE Conf. Dec. Contr.*, Orlando, FL, 2011, pp. 3331–3337.
[16] ——, "Observers for interconnected nonlinear and linear systems," *Automatica*, 2012, to appear.
[17] M. D. Shuster and S. D. Oh, "Three-axis attitude determination from vector observations," *J. Guid. Contr. Dynam.*, vol. 4, no. 1, pp. 70–77, 1981.
[18] M. Krstić, I. Kanellakopoulos, and P. V. Kokotović, *Nonlinear and Adaptive Control Design*. New York: Wiley, 1995.
[19] D. L. Kleinman and M. Athans, "The design of suboptimal linear time-varying systems," *IEEE Trans. Automat. Contr.*, vol. 13, no. 2, pp. 150–159, 1968.
[20] H. K. Khalil, *Nonlinear Systems*, 3rd ed. Upper Saddle River, NJ: Prentice-Hall, 2002.
[21] M. Chilali and P. Gahinet, "H_∞ design with pole placement constraints: An LMI approach," *IEEE Trans. Automat. Contr.*, vol. 41, no. 3, pp. 358–367, 1996.
[22] M. Chilali, P. Gahinet, and P. Apkarian, "Robust pole placement in LMI regions," *IEEE Trans. Automat. Contr.*, vol. 44, no. 12, pp. 2257–2270, 1999.

APPENDIX

The parameter projection $\operatorname{Proj}(\cdot,\cdot)$ used for the gyro bias estimation is defined as

$$\operatorname{Proj}(\hat{b},\tau) = \begin{cases} \left(I - \frac{c(\hat{b})}{\|\hat{b}\|^2}\hat{b}\hat{b}'\right)\tau, & \|\hat{b}\| \geq M_b, \quad \hat{b}'\tau > 0, \\ \tau, & \text{otherwise}, \end{cases}$$

where $c(\hat{b}) = \min\{1, (\|\hat{b}\|^2 - M_b^2)/(M_{\hat{b}}^2 - M_b^2)\}$. This is a special case of the parameter projection from Appendix E of Krstić, Kanellakopoulos, and Kokotović [18]. We recall some useful properties in the following lemma, which we state without proof.

Lemma 3: The following properties hold for the parameter projection: (i) $\operatorname{Proj}(\cdot,\cdot)$ is locally Lipschitz continuous; (ii) $\|\hat{b}\| \geq M_{\hat{b}} \implies \hat{b}'\operatorname{Proj}(\hat{b},\tau) \leq 0$; (iii) $\|\operatorname{Proj}(\hat{b},\tau)\| \leq \|\tau\|$; and (iv) $-\tilde{b}'\operatorname{Proj}(\hat{b},\tau) \leq -\tilde{b}'\tau$.